Unraveling the Role of Internal-External Metal Substitution in $Zn_3[Co(CN_6)]_2$ for Styrene Oxide-CO_2 Cycloaddition Reaction.

Erik J. Del Angel-Gómez [a], Omar Reséndiz-Hernández [a], Jesús Vega-Moreno [b], Oscar Morelos-Santos [c], Adela Lemus-Santana [a] and Benjamín Portales-Martínez [a]*.*

[a] Instituto Politécnico Nacional. CICATA Legaria, Col. Irrigación, México City, 11500, México

[b] CONAHCYT- Instituto Politécnico Nacional. CICATA Legaria, Col. Irrigación, México City, 11500, México

[c] Tecnológico Nacional de México/ Instituto Tecnológico de Ciudad Madero, Ciencias Básicas, Col. Los Mangos, Ciudad Madero, Tamaulipas, 89440, México

*bportalesm@ipn.mx and *alemuss@ipn.mx

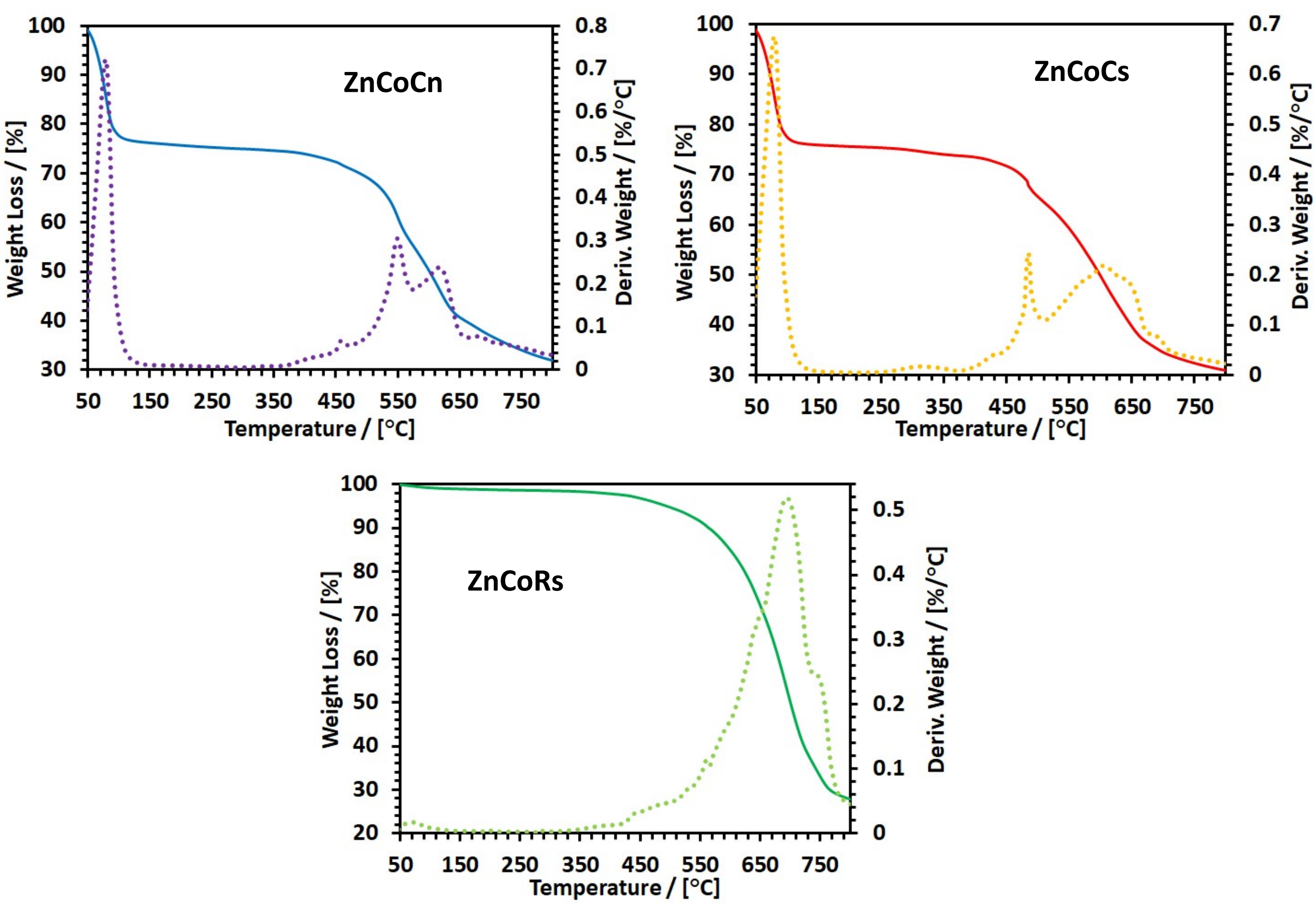

Figure S1. Thermogravimetric performance of 3 materials.

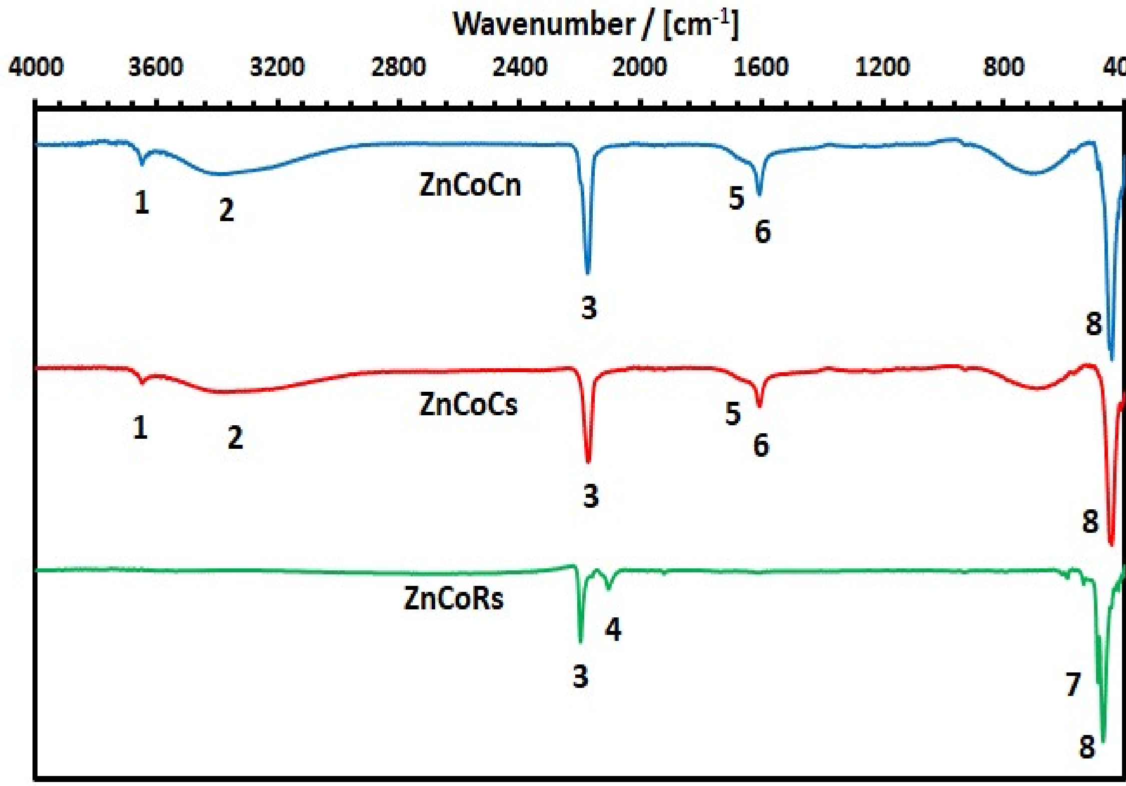

Figure S2. Infrared spectra of a) Cubic (F-43m) $Zn_3[Co(CN)_6]_2{\cdot}12H_2O$; b) cubic stabilized (Pm-3m) $Zn_{2.7}Cd_{0.3}[Co(CN)_6]_2{\cdot}12H_2O$; c) Rhombohedral stabilized (R-3c) $Zn_3[Fe_{0.1}Co_{0.9}(CN)_6]_2$.

The band in 3,650 cm^{-1} (**1**) is due to the asymmetric vibration of water molecules that are coordinated to Zn atoms; the wide band from 3,570 to 2,900 cm^{-1} (**2**) originates from the combination of asymmetric and symmetric vibrations of the hydrogen bridged water molecules; the band in 2,175 cm^{-1} (**3**) is the stretching vibration of triple bonded carbon to nitrogen in the cyanide block $[Co(CN)_6]^{-3}$; the band in 2,106 cm^{-1} (**4**) is stretching vibration of CN in $[Fe(CN)_6]$; the band forming a shoulder in 1,675 cm^{-1} (**5**) is for the bending vibration of the hydrogen bridged water molecules; the band in 1,609 cm^{-1} (**6**) is for the bending vibration of water molecules that are coordinated to Zn atoms; the band in 488 cm^{-1} (**7**) is due to the bending vibration of Fe-C≡N- atoms; the band in 471 cm^{-1} (**8**) is for the bending vibration of Co-C≡N- chain.

Table S1. Crystallographic Parameter of catalysts

	ZnCoCn	**ZnCoCs**	**ZnCoRs**
Geometry	Cubic	Cubic	Rhombohedral
space group	F -4 3 m	P m -3 m	R -3 c
H_2O molecules	12	12	0
a [Å]	10.252	10.287	12.478
b [Å]	10.252	10.287	12.478
c [Å]	10.252	10.287	32.738
External* Vacancy [%]	26.37	25	0
Internal Vacancy [%]	50.56	49.56	0
Size (Å)	1128.68	740.23	1778.51
Strain (%%)	6.87	34.28	1.94

*****Zn or Cd; **‘**Co or Fe

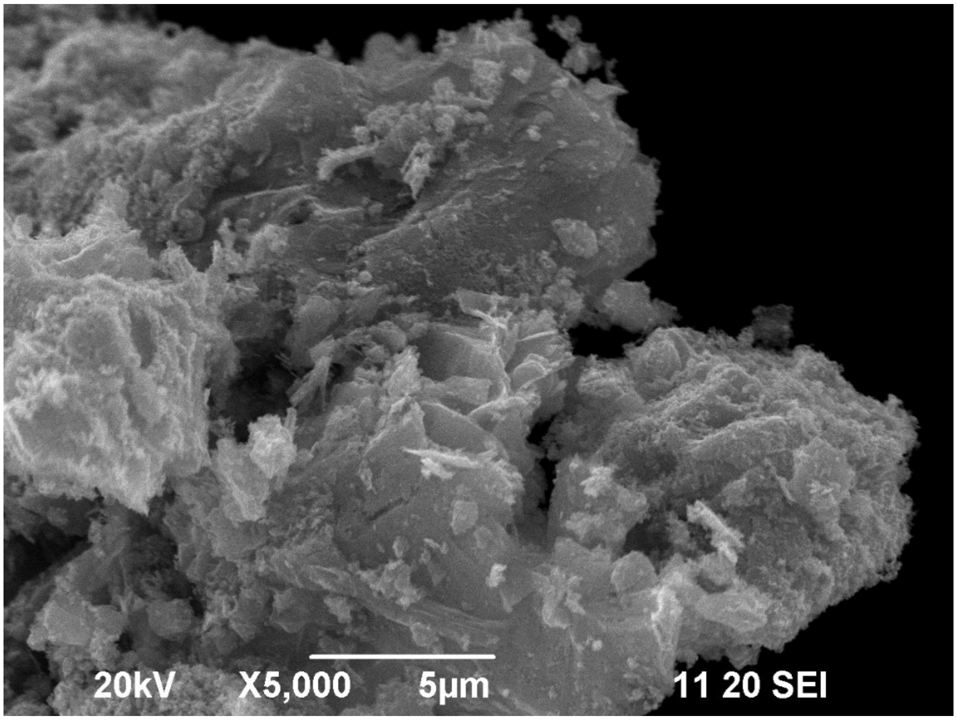

Figure S3. SEM image of zinc hexacyanocobaltate (III) (ZnCoCn), there is a big particle with the smallest ones above.

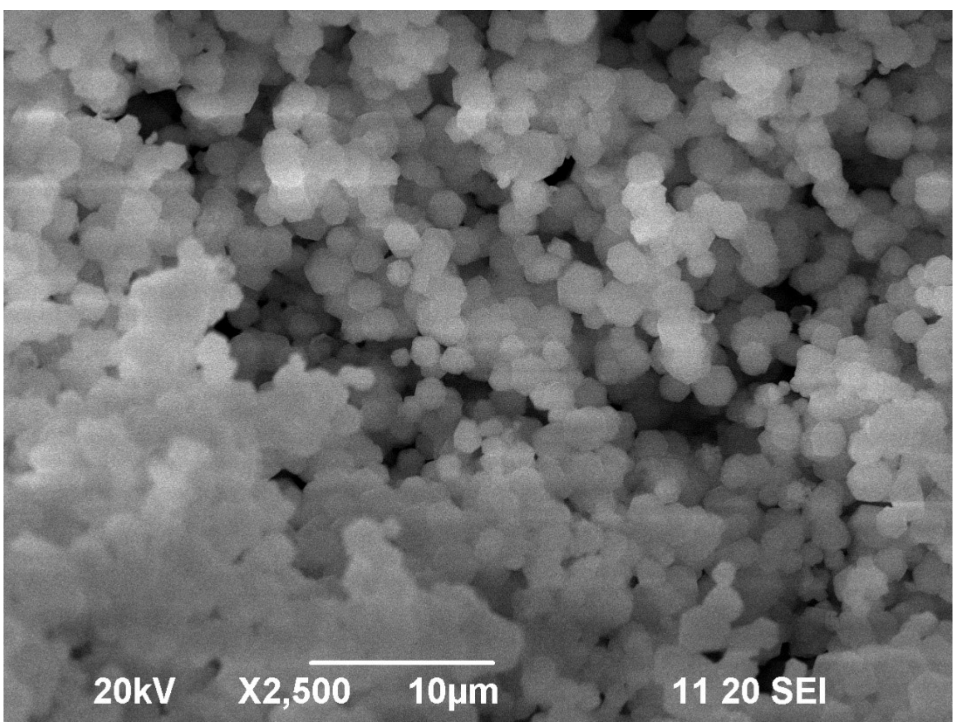

Figure S4. SEM image of zinc-cadmium hexacyanocobaltate (III) (ZnCoCs).

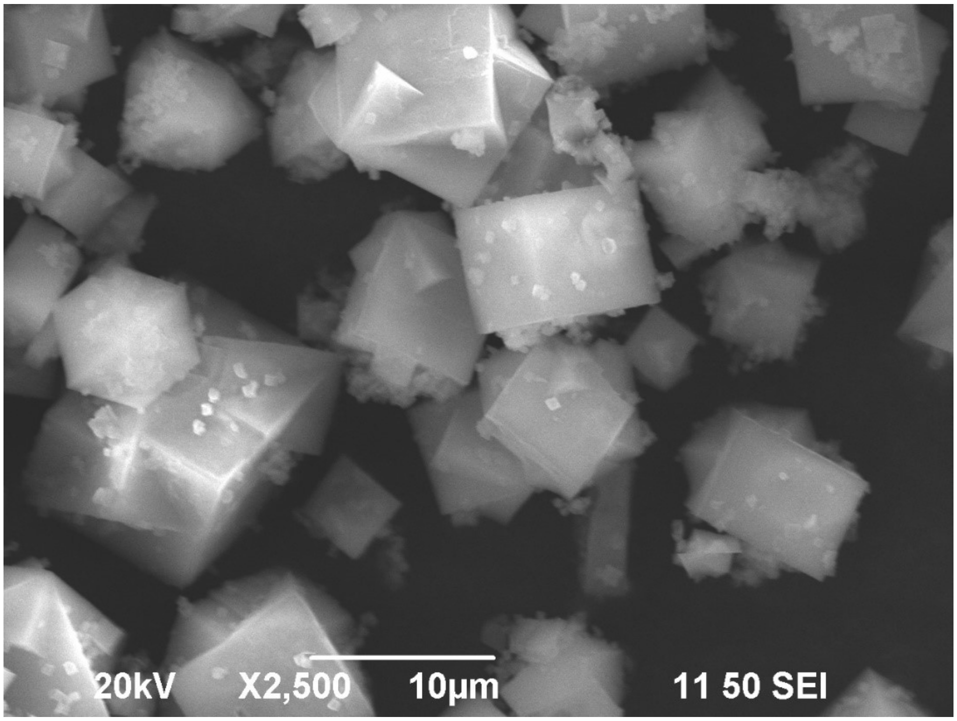

Figure S5. SEM image of zinc hexacyanocobaltate with iron replacement (III) (ZnCoRs).

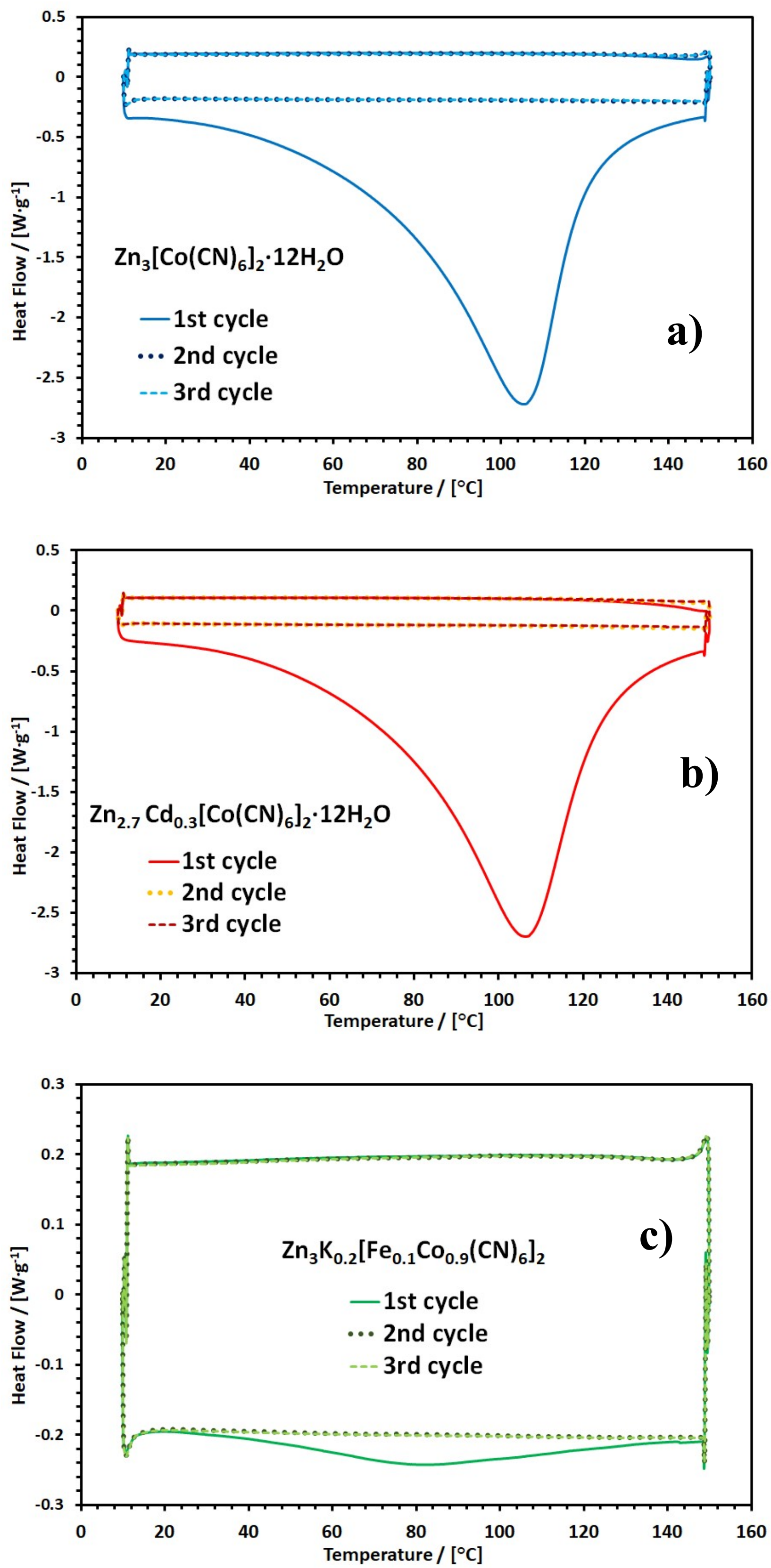

Figure S6. 3-cycle DSC Termogram of catalysts: **a)** ZnCoCn (1^{st} cycle) and ZnCoRn (2^{nd} and 3^{rd} cycle); **b)** ZnCoCs; **c)** ZnCoRs.

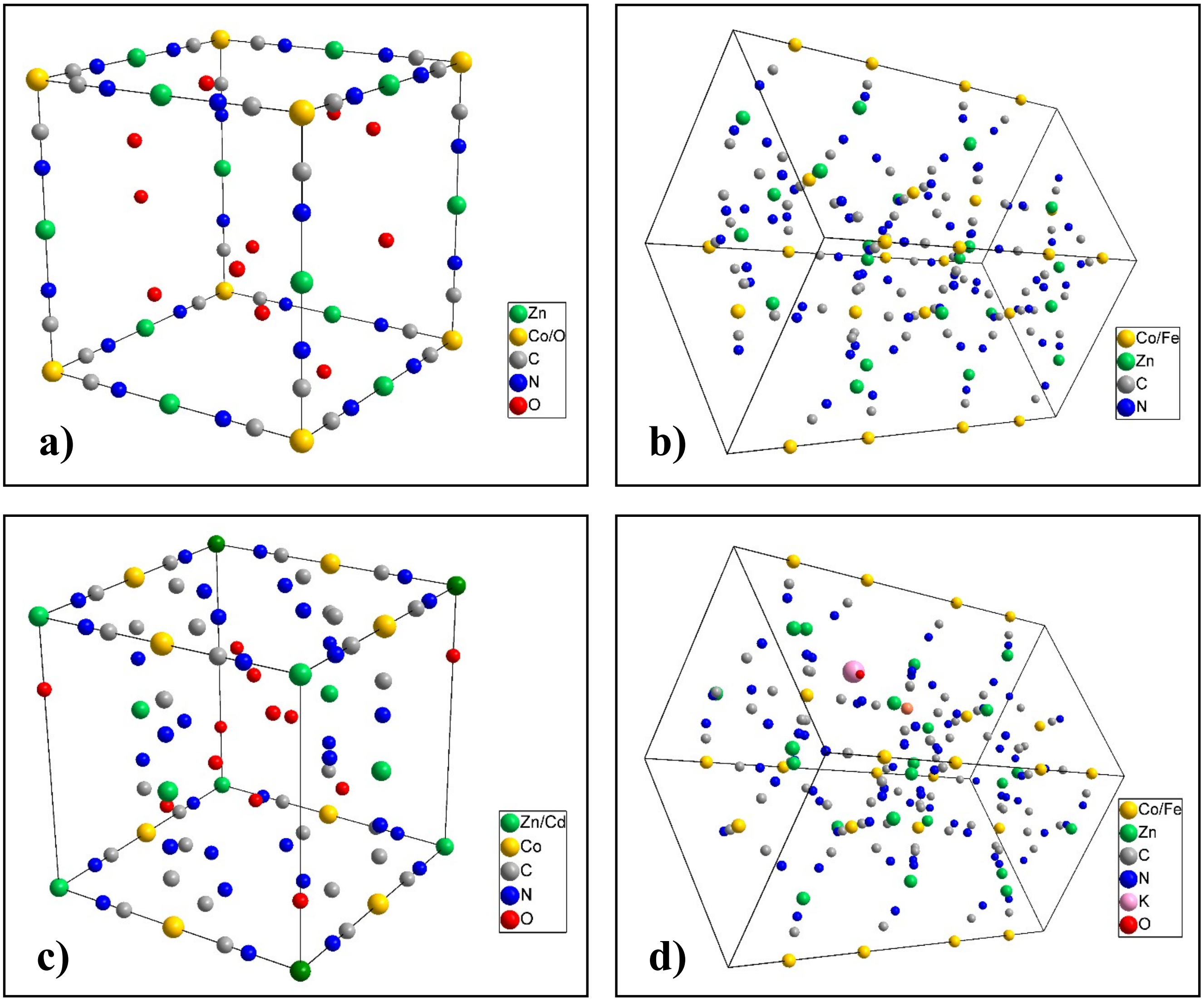

Figure S7. Unity Cell image of zinc hexacyanocobaltates; a) Cubic F -4 3 m $Zn_3[Co(CN)_6]_2 \cdot 12H_2O$, the red balls are the distinct water molecules; b) Rhombohedral R -3c; c) cubic P m -3 m stabilized, the darker cyan balls are cadmium atom and red balls the water; d) Rhombohedral R -3 c stabilized, the orange balls are the internal iron, the green one is the potassium as compensation cation and red are the water associated.

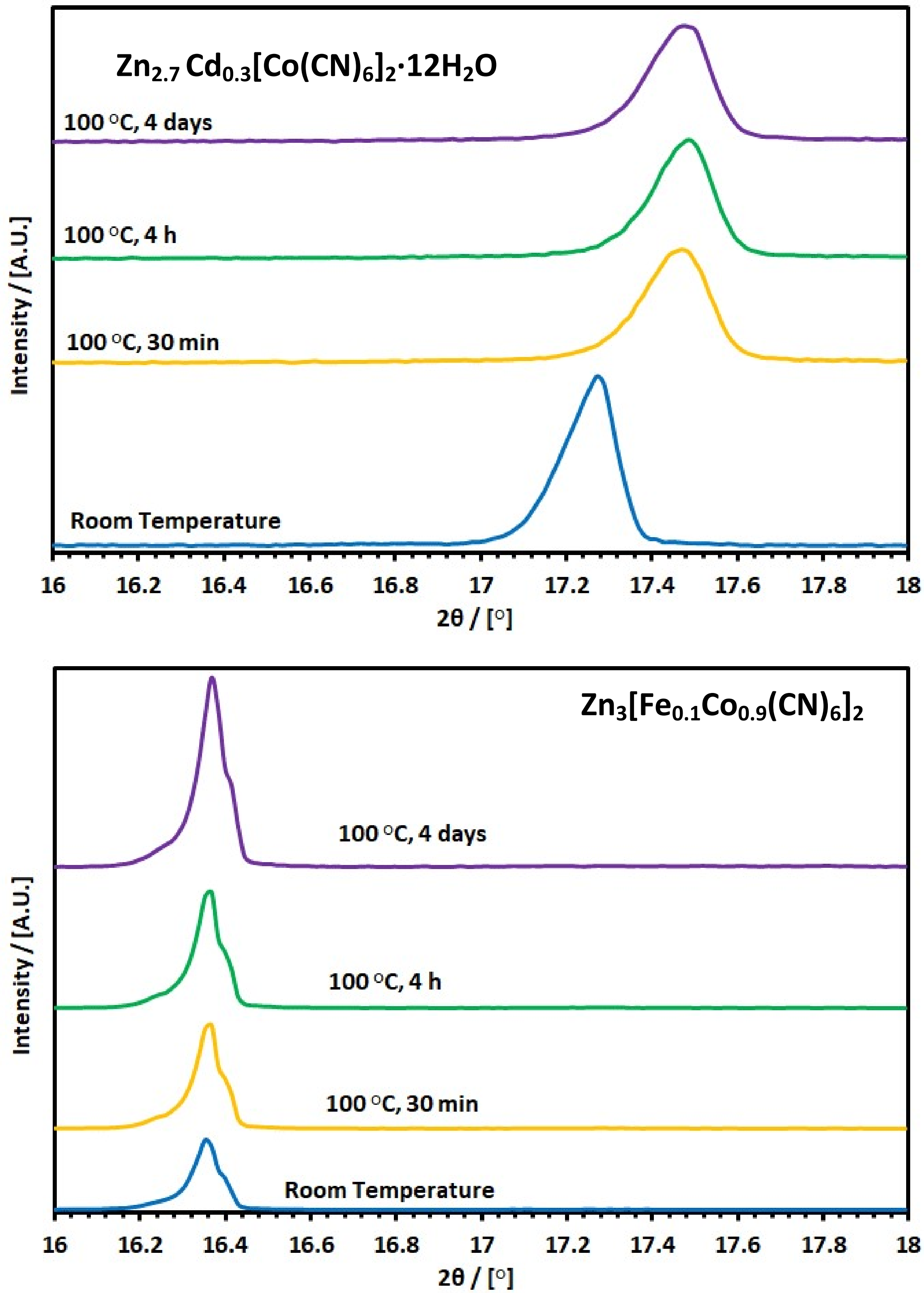

Figure S8. Thermal treatment at different times to water extraction in stabilized materials.

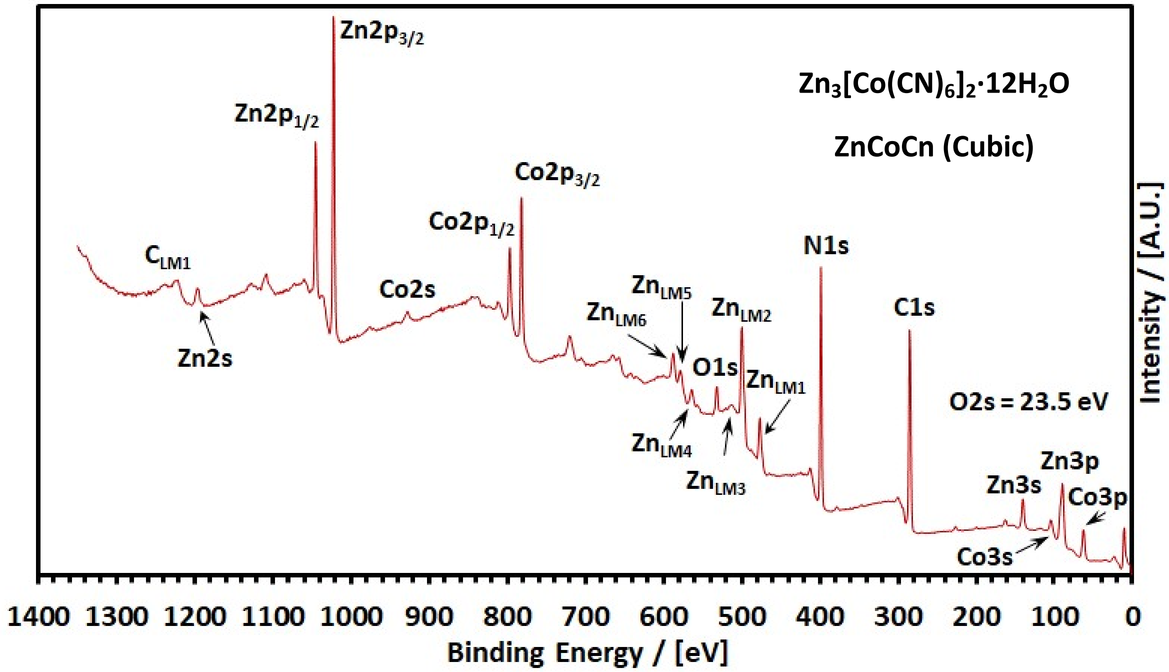

$Zn_3[Co(CN)_6]_2 \cdot 12H_2O$
ZnCoCn (Cubic)
$Zn2p_{3/2}$
$Zn2p_{1/2}$
$Co2p_{3/2}$
$Co2p_{1/2}$
C_{LM1}
Co2s
Zn2s
Zn_{LM5}
Zn_{LM6}
Zn_{LM2}
O1s
Zn_{LM1}
Zn_{LM4}
Zn_{LM3}
N1s
C1s
O2s = 23.5 eV
Zn3p
Zn3s
Co3p
Co3s
1400 1300 1200 1100 1000 900 800 700 600 500 400 300 200 100 0
Binding Energy / [eV]
Intensity / [A.U.]

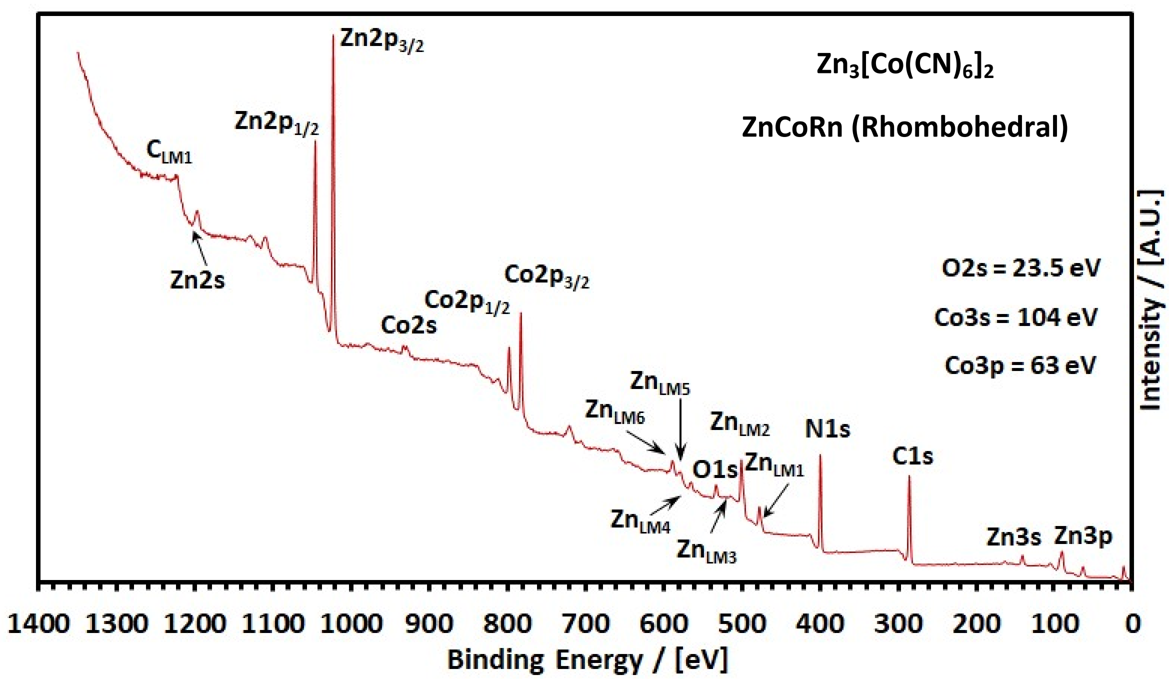

$Zn_3[Co(CN)_6]_2$
ZnCoRn (Rhombohedral)
$Zn2p_{3/2}$
$Zn2p_{1/2}$
C_{LM1}
Zn2s
$Co2p_{3/2}$
$Co2p_{1/2}$
Co2s
O2s = 23.5 eV
Co3s = 104 eV
Co3p = 63 eV
Zn_{LM5}
Zn_{LM6}
Zn_{LM2}
N1s
C1s
O1s
Zn_{LM1}
Zn_{LM4}
Zn_{LM3}
Zn3s
Zn3p
1400 1300 1200 1100 1000 900 800 700 600 500 400 300 200 100 0
Binding Energy / [eV]
Intensity / [A.U.]

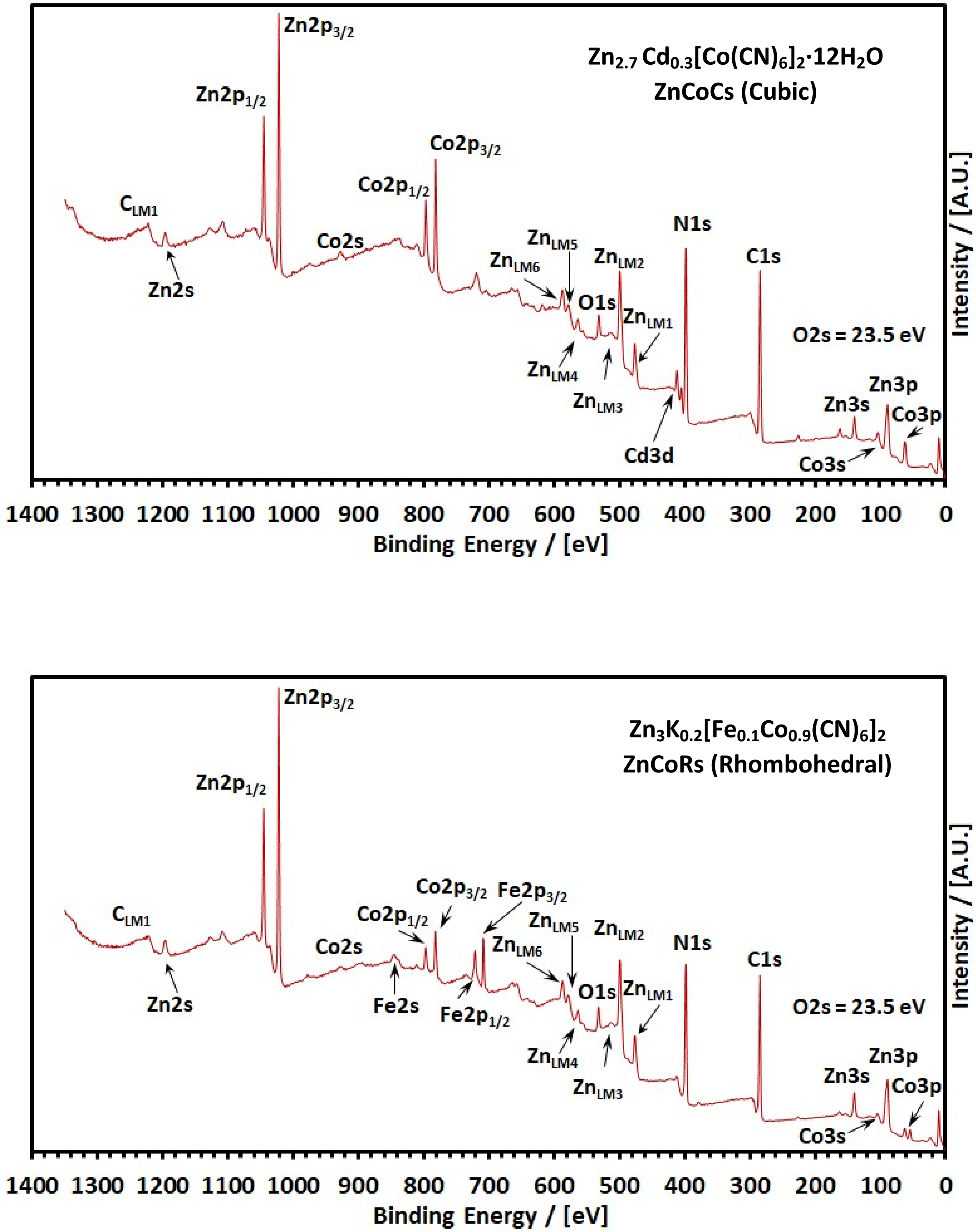

Figure S9. XPS survey spectra of all materials.

Table S2. C 1s, N 1s, Co 2p, and Zn 2p BE (eV) and Zn Auger (kinetic energy in eV) and Auger modified parameter of the catalysts.

	C $1s_{CN}$	N $1s_{Zn-N}$	Co $2p_{3/2}$	Zn $2p_{3/2}$	Zn $L_3M_{45}M_{45}$	α'_{Zn} [eV]
ZnCoCs	284.39	397.8	781.29	1021.4	987.55	2008.95
ZnCoCn	284.41	397.66	781.15	1021.29	987.6	2008.89
ZnCoRn	284.42	397.7	781.32	1021.33	987.7	2009.03
ZnCoRs	284.37	397.4	782.19	1021.75	987.6	2009.35

Because auger peaks have well-defined positions and shapes (see Figure S9 in supporting information), the zinc auger line $L_3M_{45}M_{45}$ was measured (Table S2), due to Zn^o and ZnO having a narrow binding energy difference (0.65 eV) [53].

Taking the cubic phase (ZnCoCn) as a reference, the rhombohedral phase shows an +0.1 eV shift, in agreement with Zn $2p_{3/2}$ results, the cubic stabilized presented a negligible decrease of 0.05 eV and the rhombohedral stabilized has no change. Hence, the modified Auger parameter (α') [48,56,57] was calculated to find a better way to determine the Zn chemical environment, as compared above, taking the cubic phase (ZnCoCn) as a reference with 2008.89 eV (calculated), the rhombohedral phase has a +0.14 eV shift, according with the previous discussed, due to the positive charge accumulation in Zn atom by the change to tetrahedral coordination and water molecules loss. The cubic stabilized showed a +0.06 eV shift, opposite of what was found in the auger peak, but keeping in mind that the modified auger parameter is a combination of the kinetic energy of $L_3M_{45}M_{45}$ Auger line and $2p_{3/2}$ peak, the net effect for chemical environment analysis is sensed [48,56,57], becoming the best option because has no charge effect interference, for this reason, the α' was chosen for the final Zn analysis, the result may be attributed to the cadmium atoms that replace zinc in 9:1 proportion as was determined by XRD (see Figure S7-c), a unit cell) and the rhombohedral stabilized phase presented a +0.46 shift, due to the iron substitution as an internal metal, as discussed before, iron is slightly less electronegative than cobalt, then the π-back bonding charge donation effect has more positive charge accumulation in zinc atoms.

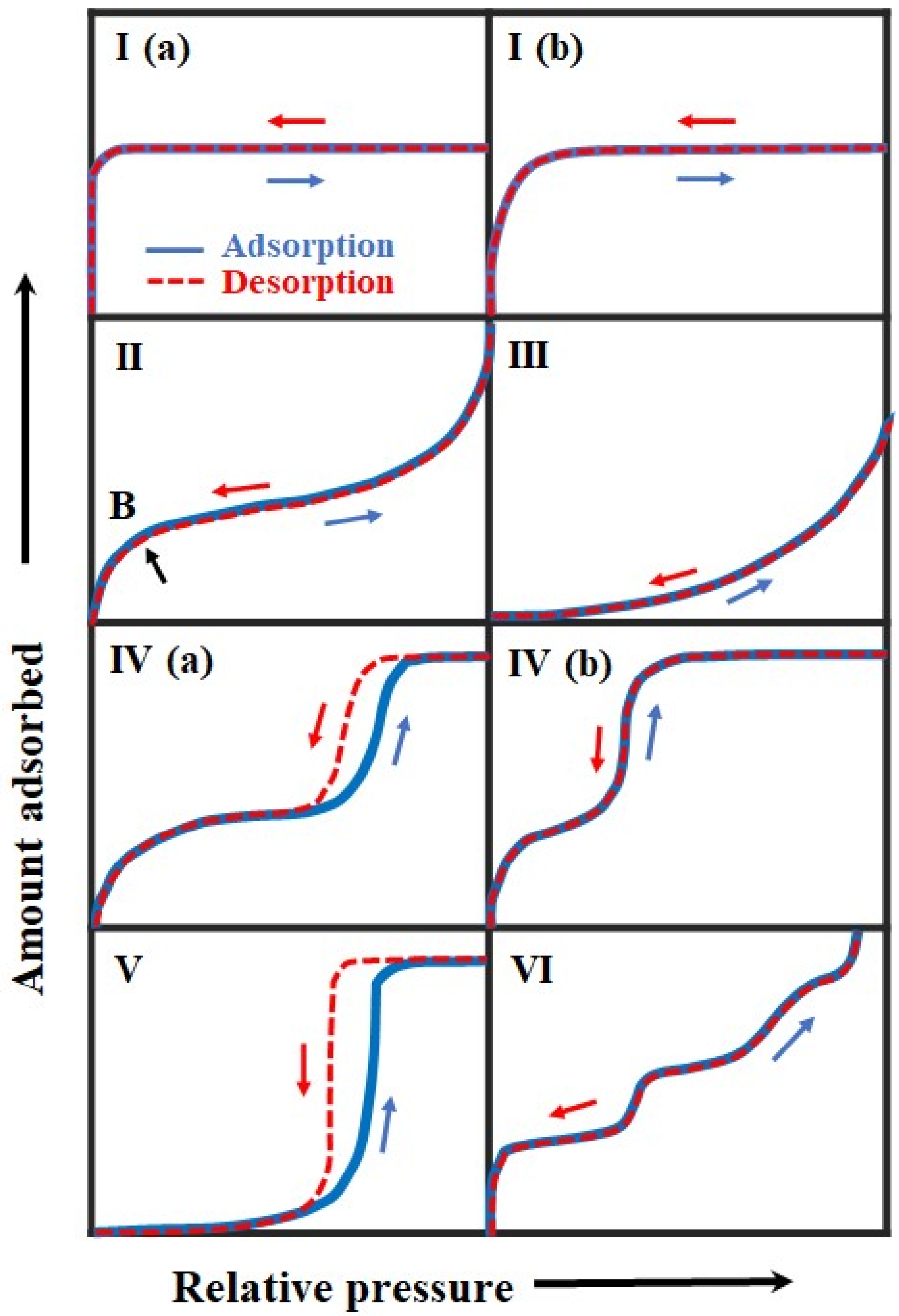

Figure S10. IUPAC isotherm classification [58].

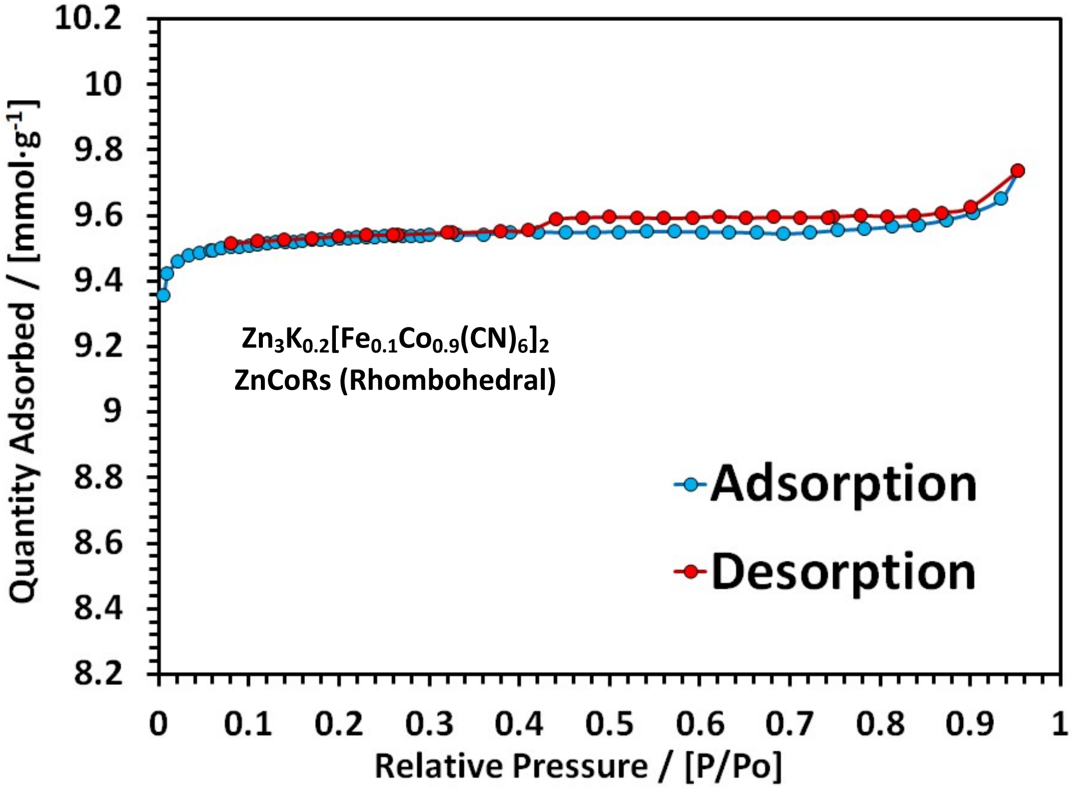

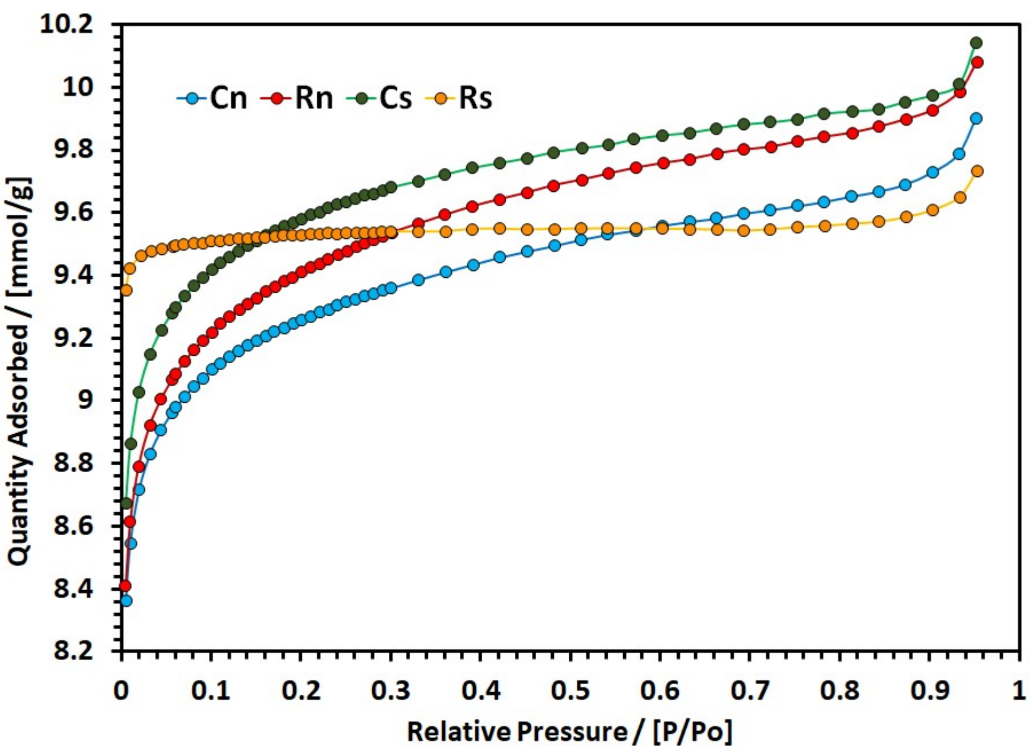

Figure S11. ZnCoRs Isotherm comparison with other materials.

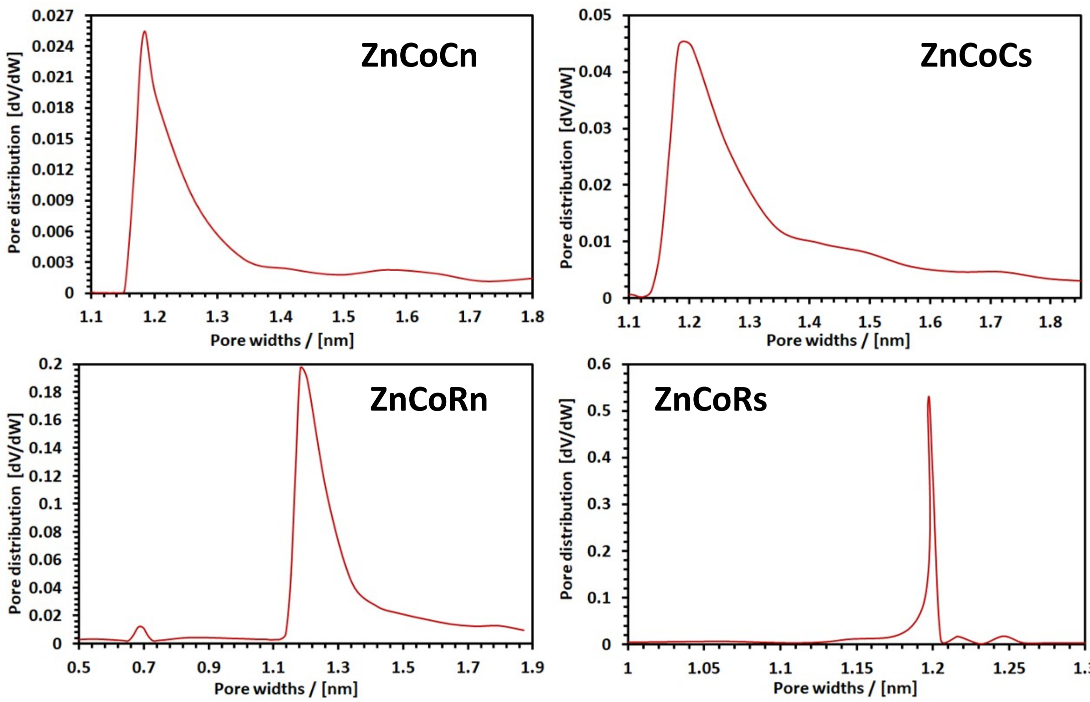

Figure S12. Micropore Size Distribution calculated by the DFT method.

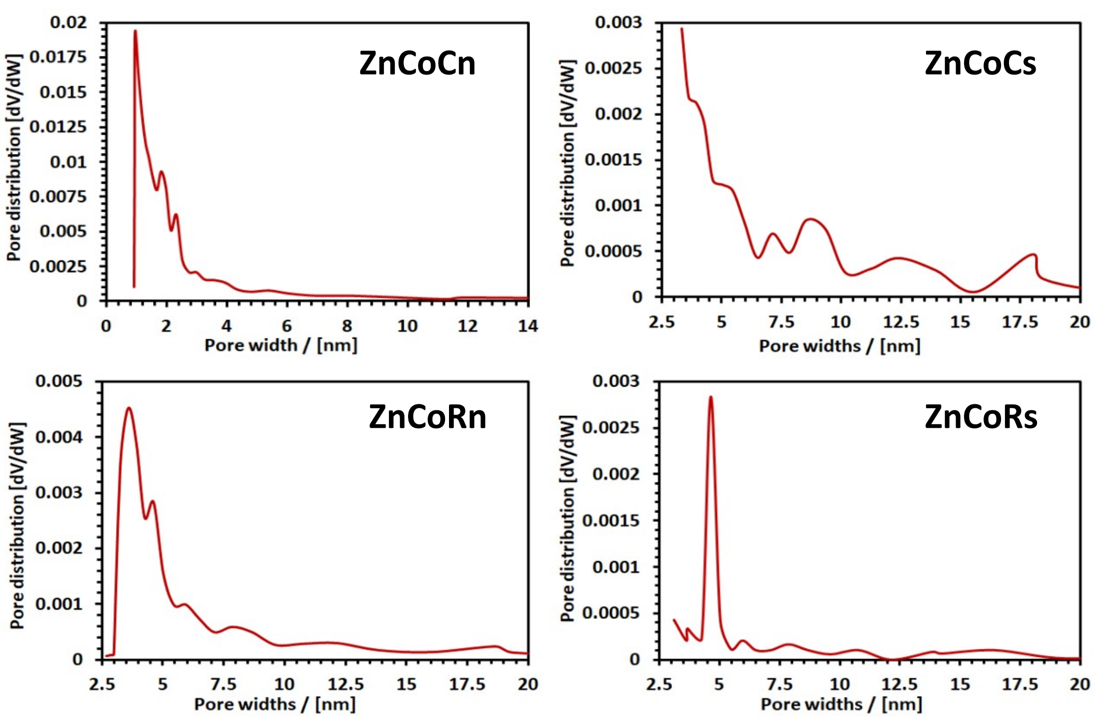

Figure S13. Mesopore Size Distribution calculated by BJH method.

Table S3. Textural properties of all studied materials

	ZnCoCn	**ZnCoRn**	**ZnCoCs**	**ZnCoRs**
BET Surface Area ($m^2 \cdot g^{-1}$)	624.86	636.94	646.28	634.52
t-Plot Micropore Area ($m^2 \cdot g^{-1}$)	552.8	550.52	574.1	625.79
t-Plot External Area ($m^2 \cdot g^{-1}$)	72.05	86.43	72.18	8.73
Pore Volume ($cm^3 \cdot g^{-1}$)	0.343	0.349	0.351	0.337
t-Plot micropore vol. ($cm^3 \cdot g^{-1}$)	0.289	0.288	0.3	0.326
Micropore Size by DFT (Å)	11.82	11.82	12.04	11.96
Mesopore Size by BJH (Å)	26.082	25.662	24.999	32.117

^{1}H NMR characterization

The spectra were recorded with a Bruker Ascend 750 MHz spectrometer with a relaxation time of 10 s and a 2 mM hexamethyldisilane (HMDS), in the NMR laboratory of the Centro de Nanociencias y Micro y Nanotecnologías (CNMN) of the Instituto Politécnico Nacional.

Table S4. ^{1}H NMR signals of the mixture obtained for ZnCoCn in 2 h reaction.

Chemical shift (ppm)	Type	Molecular group	Proton	Compound
0.04	Singlet	CH_3	$-Si-CH_3$	HMDS
1.01	Triplet	CH_3	$-CH_2-CH_3$	TBAB
1.46	Sextuplet	CH_2	$-CH_2-CH_2-CH_3$	TBAB
1.68	Quintuplet	CH_2	$-CH_2-CH_2-CH_2-$	TBAB
2.8	Double doublet	CH_2	$-CH-CH_2-O-$	Styrene oxide
3.15	Double doublet	CH_2	$-CH-CH_2-O-$	Styrene oxide
3.38	Triplet	CH_2	$-N^{+}-CH_2-CH_2-$	TBAB
3.67	Double doublet	CH_2	$-CH-CH_2-OH$	Alcohol
3.76	Double doublet	OH	$-CH_2-OH$; $-CH-OH$	Alcohol
3.86	Triplet	CH	$-O-CH-CH_2-$	Styrene oxide
4.24	Double doublet	CH_2	$-CH_2-CH-$	Polycarbonate
4.34	Double doublet	CH_2	$-CH-CH_2-O-$	Styrene carbonate
4.44	Double doublet	CH_2	$-CH_2-CH-$	Polycarbonate
4.69	Double doublet	CH_2	$-CH_2-CH-$	Copolymer
4.8	Double doublet	CH_2	$-CH-CH_2-O-$	Styrene carbonate
4.83	Triplet	CH	$-CH_2-CH-OH$	Alcohol
4.9	Double doublet	CH_2	$-CH_2-CH-$	Copolymer
5.57	Triplet	CH	$-CH_2-CH-$	Copolymer
5.67	Triplet	CH	$-O-CH-CH_2-$	Styrene carbonate
5.77	Triplet	CH	$-CH_2-CH-$	Polycarbonate
6.70-8.20	-	C_6H_5	C_6H_5-	Reagent and products

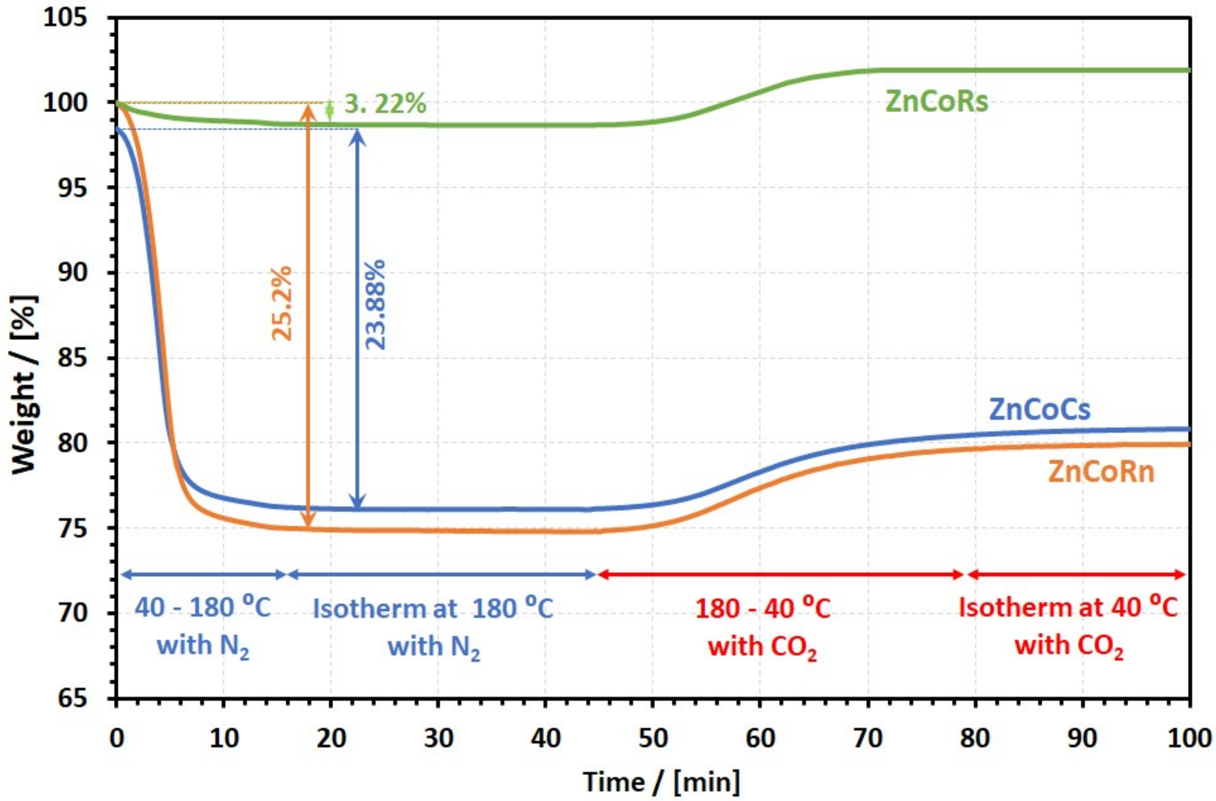

Figure S14. TGA experiment with 25 ml·min^{-1} of CO_2 flow.

The experiment was carried out first with 25 ml·min^{-1} of N_2 flow and an isothermal range was performed, to probe if any interaction may occur, then, the flow was changed to CO_2. And lets the temperature down to 40 °C by the thermal equilibrium.

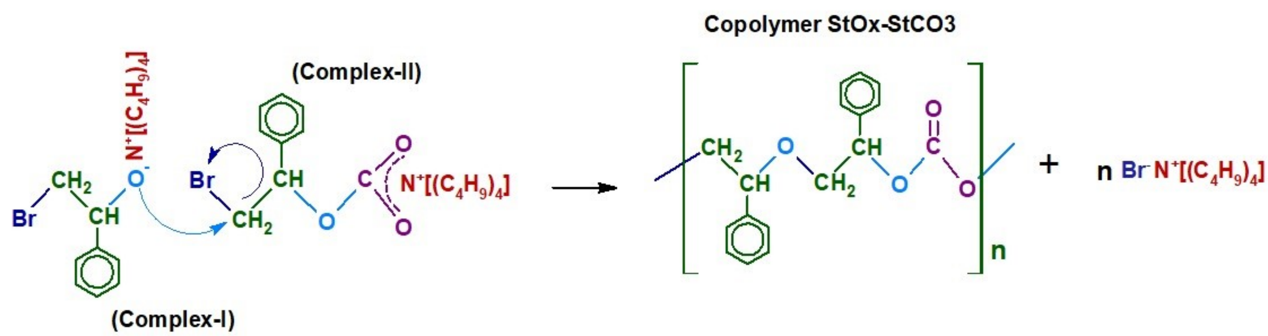

Figure S15. Copolymer formation.

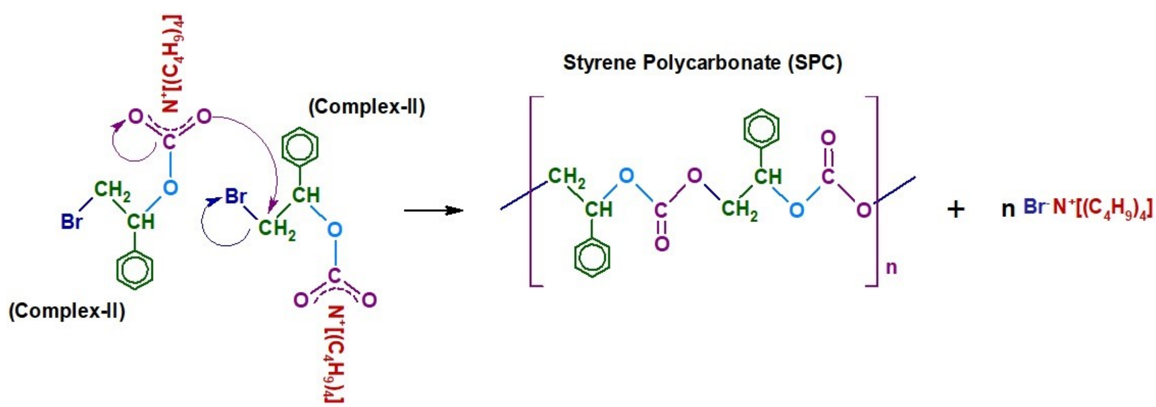

Figure S16. Styrene Polycarbonate formation.

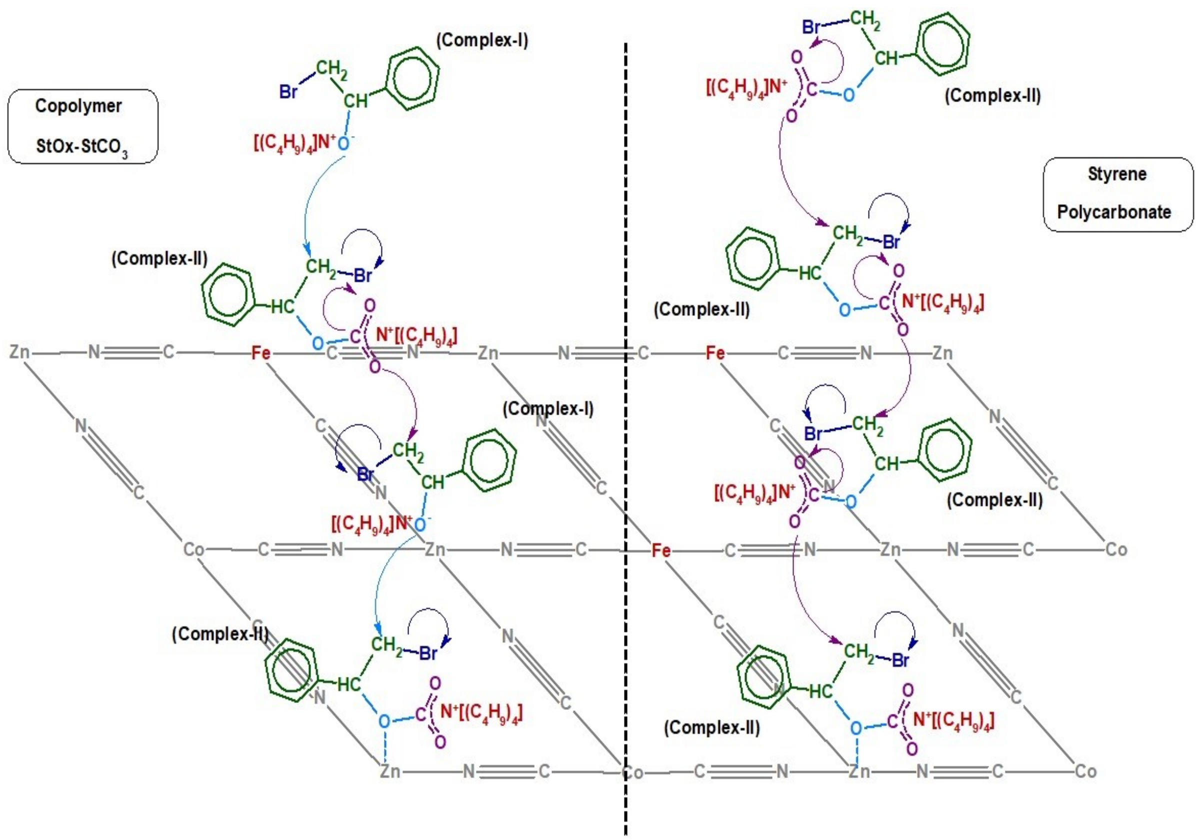

Figure S17. Copolymer and Styrene Polycarbonate formation on ZnCoRs surface.